Available online at www.sciencedirect.com
SCIENCE DIRECT®
Journal of Chromatography A, 1044 (2004) 97–111
JOURNAL OF CHROMATOGRAPHY A
www.elsevier.com/locate/chroma

Review

Chip electrochromatography

Timothy B. Stachowiak [a], Frantisek Svec [b,*], Jean M.J. Fréchet [a,b]

[a] *Department of Chemical Engineering, University of California, Berkeley, CA 94720-1460, USA*
[b] *Department of Chemistry, University of California, Berkeley, CA 94720-1460, USA*

Available online 15 June 2004

Abstract

Electrochromatography (EC) in microfluidic chips is emerging as an attractive alternative to capillary electrophoresis (CE) for on-chip separations. This review summarizes recent developments in the rapidly growing area of chip electrochromatography with a focus on "column" technologies. Relevant achievements are summarized according to the types of stationary phase used for the separations including open channels, microfabricated structures, and channels packed with beads or containing a porous monolith. The advantages and disadvantages of each, as well as practical aspects of their application, are discussed. The analytical performance of these devices is demonstrated with separations involving various families of compounds mostly in the reversed-phase chromatographic mode.

Keywords: Reviews; Electrochromatography; Chip technology; Stationary phase, electrochromatography

Contents

1. Introduction

High-performance separation systems are critical to the success of micro-total analysis systems (μ-TAS). Yet, at the present time, on-chip separations are dominated by capillary electrophoresis (CE) and other electrophoretic methods. However, as the field of μ-TAS develops there is a growing demand for additional modes of separation, especially chromatographic modes, in order to better handle increasingly complex samples. Emerging research areas, such as proteomics, require the use of multi-dimensional separations in order to fully resolve complex mixtures of proteins and/or peptides.

A promising alternative to capillary electrophoresis is electrochromatography, a technique that includes features of both electrophoresis and liquid chromatography. As is the case in electrophoresis, a voltage applied across the separation device drives the samples through the system via electroosmotic flow (EOF). However, in analogy to liquid chromatography, the separation device contains a solid stationary phase. Therefore, electrochromatographic separations are achieved as a result of differences in both electrophoretic mobility (for ionized analytes) and specific interactions of

* Corresponding author. Tel.: +1 510 643 3168; fax: +1 510 643 3079.
E-mail address: svec@uclink4.berkeley.edu (F. Svec).

0021-9673/$ – see front matter © 2004 Elsevier B.V. All rights reserved.
doi:10.1016/j.chroma.2004.04.075

solutes with the stationary phase. This combination of separation mechanisms enables the efficient electrochromatographic separation of both ionizable and neutral compounds.

One of the major advantages of electrochromatography (EC) compared to HPLC is the relative ease with which it can be miniaturized into a microfluidic chip format. The separation in EC mode is achieved by simply applying an electric field across the channel. Since the fluid flow is driven by EOF, the separation device need not include mechanical pumps or valves [1]. In addition, the flat flow profile generated by EOF minimizes dispersion of analyte bands during their passage through the stationary phase, allowing very high plate counts to be achieved. Since EOF is largely independent of channel or particle size, both small size beads or monolithic stationary phases with very small pores can be used, facilitating solute mass transfer without generating the large pressure drops associated with the same materials in classical HPLC.

Although several excellent reviews covering the broad area of separations in μ-TAS include brief discussions of electrochromatography [2–8], this review is the first we are aware of dedicated to chip electrochromatography. Despite remarkable progress, this field is still in its infancy. Therefore, it is our intention to present a review of the relevant literature that is as complete as possible. A great deal of the work in this field has been dedicated to developing and/or demonstrating different methods that enable the introduction of stationary phase within the channels of a microfluidic device. Consequently, we have arranged the studies summarized in this review according to the type of stationary phase used within the microchip channel.

2. Open channel electrochromatography

2.1. Glass chips

The earliest studies of on-chip electrochromatography utilized open channels with chemically modified walls serving as the stationary phase. Ramsey and coworkers demonstrated the first such separation on a glass microchip with a 16.5 cm long serpentine channel that was 5.6 μm deep and 66 μm wide [9]. The walls in this channel were modified with octadecyltrichlorosilane in a pressurized, high-temperature process to afford a C_{18} surface chemistry. The reversed-phase separation of three neutral coumarin dyes using 5.8 cm of the channel length was achieved in less than three minutes, with a separation efficiency of up to 11 700 plates (200 000 plates/m).

Later, several improvements were made to this open channel chip electrochromatography (OChEC) microchip, including a shorter, straight separation channel, a mixing tee for solvent programming, and an improved octadecylsilane modification procedure carried out at room temperature [10]. Microchannels with the C_{18} coating exhibited a decrease of 10–25% in electroosmotic flow compared to similar, non-coated channels. This effect was measured in six devices with different channel geometries. No apparent correlation between geometry and extent of EOF reduction was found. The effect of channel depth on separation performance for channels 2.9–10.2 μm deep was also investigated. Not surprisingly, shallower channels afforded higher efficiencies due to reduced mass transfer limitations. In addition, the minima of the Van Deemter plots shifted to higher linear velocities with decreased channel depth. This confirmed that highly efficient separations could be carried out very rapidly in shallow open channels. However, only small improvements in plate heights were observed for channels less than about 5 μm deep. For this reason and also because the fabrication and operation of very shallow channels is difficult, 5 μm deep channels were used for the remainder of the study. The aforementioned improvements to the microchip design significantly enhanced the performance for a separation of four coumarin dyes. Even under isocratic conditions, plate counts increased by one order of magnitude compared to the first microchip design. Although the mixture of coumarins was well resolved under these conditions, gradient elution further narrowed the peak width, increased the signal-to-noise ratio, and reduced analysis time. Under optimized conditions, the four coumarins were eluted within a 6 s window and the chromatographic run was completed in less than 20 s. As shown in Fig. 1, a steep gradient of acetonitrile in aqueous buffer solution was used, with acetonitrile content increasing from 29 to 50% in 5 s.

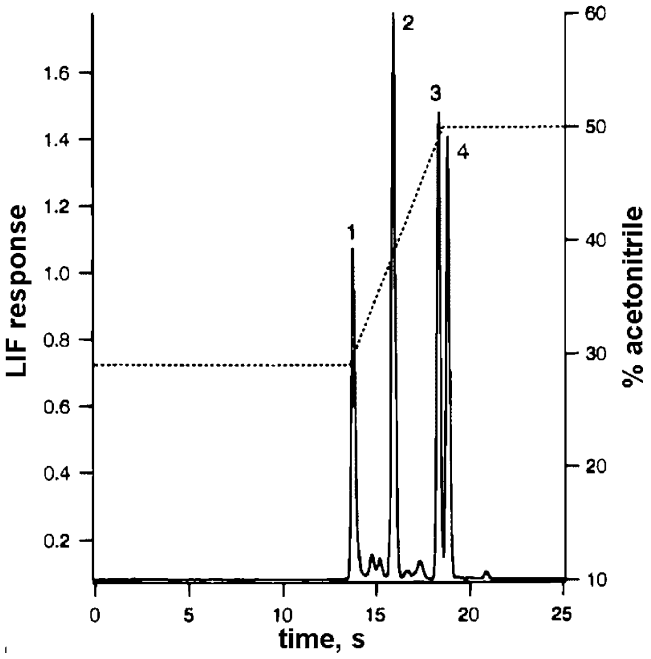

Fig. 1. Fast open channel electrochromatography on a microchip. Channel depth, 5.2 μm; stationary phase coating, octadecylsilane; mobile phase, 10 mM borate buffer (pH 8.4) with a linear gradient of acetonitrile from 29 to 50% within 5 s, starting 1 s after injection; analytes, (1) coumarin 440, (2) coumarin 450, (3) coumarin 460, and (4) coumarin 480; field strength, 700 V/cm; dotted line, gradient trace. From Ref. [10] with permission.

A third-generation of open channel devices integrated filtration, preconcentration, and OChEC separation with solvent programming into a single microchip [11]. During operation, this multifunctional device filtered the solution by passing fluid through seven 1 μm deep channels at the entrance to the chip. Both sample concentration and separation were performed in a C_{18}-modified analysis channel that was 5 μm deep and 22 μm wide. Solid-phase extraction experiments using a 900 nmol/L solution of pyrene achieved signal enhancement factors as high as 400. To demonstrate the separation performance of the device, a mixture of four polycyclic aromatic hydrocarbons (PAHs) was loaded onto the front end of the stationary phase coating and then eluted in the reversed-phase mode using a stronger mobile phase with higher acetonitrile content. The device afforded excellent efficiencies, with three of the four PAHs having plate heights of 1.16 μm or less. Unfortunately, the high performance was only achieved for small volumes of injected sample since the low surface area of the wall coating limited the loading capacity of the device. Fig. 2 illustrates that the quality of the separation significantly degraded at long injection times for some of the analytes because the column loading capacity was exceeded.

Targeting high-peak capacity applications, which are important for the separation of complex mixtures such as those in proteomic studies, open channel electrochromatography was combined with CE to create a two-dimensional (2D) microchip separation system [12]. The chip, shown in Fig. 3, contained a 25 cm spiral OChEC channel interfaced with a 1.2 cm CE channel. Using 0.2 s long "gated" injections, effluent from the first dimension OChEC channel was repetitively injected into the CE channel every 3.2 s. Approximately 9% of the total volume of effluent from the first dimension separation was injected into the second dimension channel. To demonstrate the capabilities of this system, the TRITC-labeled tryptic digest of β-casein was separated using the 2D microchip system. The resulting chromatogram, which was obtained in under 13 min, is shown in Fig. 4. Performance of the microchip was somewhat limited by the incomplete orthogonality of the two dimensions since electrochromatographic separation is also affected by electrophoretic mobility. This overlap of separation mechanisms reduced the overall peak capacity of the system. In addition, in order to achieve a representative injection from the first dimension into the second dimension, the sampling rate should enable multiple injections from each first dimension peak, ideally four or more, into the second dimension CE channel. However, the average rate of sample introduction into the second dimension in this study was at most two injections per first dimension peak. Despite these limitations, a significant increase in the number of distinguishable peaks, from 17 to 26, was achieved compared to a single dimension OChEC separation under the same conditions.

Open channel stationary phases have also been created using techniques other than silanization. For example, sol–gel chemistry was used to create thin silica gel coatings, which

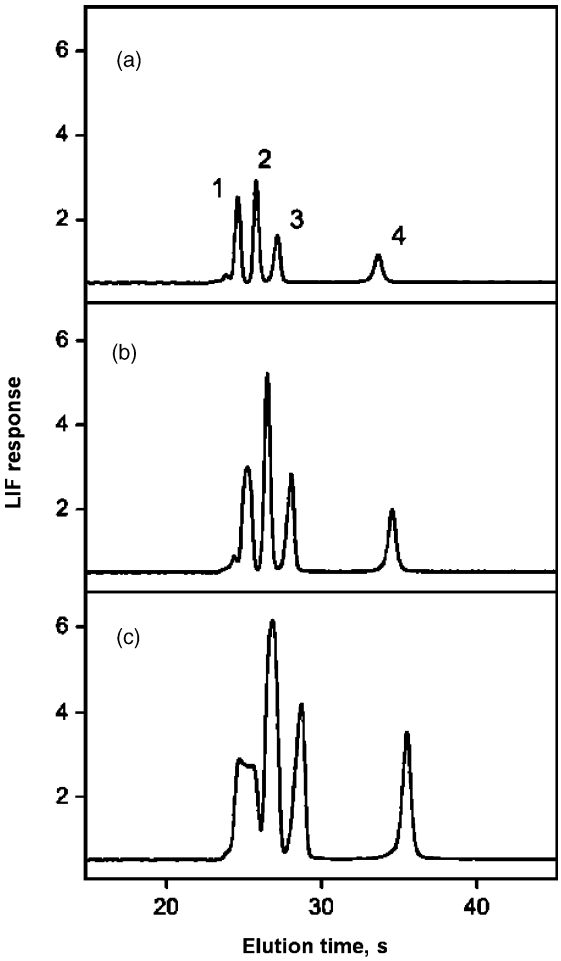

Fig. 2. OChEC separations of (1) anthracene, (2) pyrene, (3) 1,2-benzofluorene, and (4) benzo[*a*]pyrene for injection times of (a) 80 s, (b) 160 s, and (c) 320 s. A step gradient of 10 mM Tris buffer beginning at 52% (v/v) acetonitrile, holding for 10 s, and then switching to 56% (v/v) acetonitrile was used. The field strength in the analysis channel was 500 V/cm and the stationary phase coating was octadecylsilane. The concentrations of analytes 1–4 were 2.8, 0.9, 5.8, and 5.0 μM, respectively. From Ref. [11] with permission.

have high surface areas due to their porous structure [13]. To create these coatings, a partially gelled mixture of tetraethyoxysilane (TEOS) and *n*-octyltriethoxysilane (C_8-TEOS) was injected into the channels of a glass microchip. The silica gel was anchored to the walls of the chip through condensation reactions involving surface silanol groups. After a short reaction time, the channels were flushed with solvent to remove excess gel, leaving only a thin layer of coating on the wall surface. Finally, a sodium hydroxide wash was used to increase the surface area of the coating. Since the sol–gel mixture contained C_8-TEOS, desirable hydrophobic moieties were directly incorporated into the coating in a single reaction step. A microfluidic glass chip with a 60 cm long, 23 μm deep, and 90 μm wide serpentine channel was used for the reversed-phase separation of three PAHs. All three PAHs were baseline resolved in less than 6.5 min. Relatively low separation efficiencies were likely

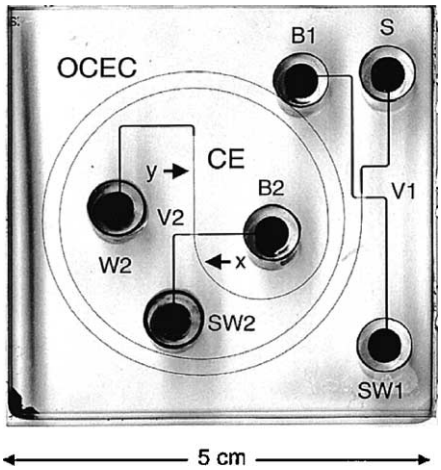

Fig. 3. Image of a microchip used for 2D separations. The separation channel for the first dimension (OChEC) extends from the first valve, V1, to the second valve, V2. The second dimension (CE) extends from the second valve, V2, to detection point *y*. Sample (S), buffer 1 and 2 (B1, B2), sample waste 1 and 2 (SW1, SW2), and waste (W) reservoirs are positioned at the terminals of each channel. The arrows indicate the detection points in the OChEC channel (*x*) and CE channel (*y*). Both channels are 10.8 μm deep and 34 μm wide. The channels and reservoirs are filled with black ink for contrast. From Ref. [12] with permission.

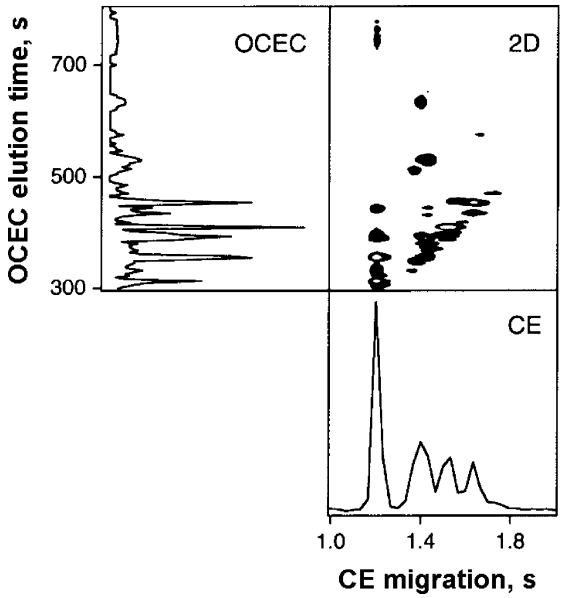

Fig. 4. 2D separation of TRITC-labeled tryptic peptides of β-casein. The projections of the 2D separation into the first dimension (OChEC) and second dimension (CE) are shown to the left and below the 2D contour plot, respectively. The field strengths were 220 V/cm in the OChEC channel and 1890 V/cm in the CE channel. The buffer was 10 mM sodium borate with 30% (v/v) acetonitrile. The fluorescence detection point, *y*, (shown in Fig. 3) was 0.8 cm past valve V2 in the CE channel. From Ref. [12] with permission.

caused by the serpentine channel geometry, large channel depth, and the use of long capillaries to interface the chip with a conventional CE instrument.

2.2. Plastic chips

While the studies discussed above were performed in glass or quartz microchips, the possibility of using microchips made of plastic has also been explored. Plastic devices are attractive as they can be mass produced rapidly and inexpensively using technologies such as injection molding or hot embossing. While the high cost of glass chips requires that they be used multiple times, mass-produced plastic microchips could potentially be used once and then discarded, thus eliminating the serious problems that could arise from cross-contamination and sample carryover for multiple use devices.

The modification of glass channel walls using silane chemistry is well established. In contrast, modification strategies for polymer substrates are still being developed. For example, a two-step procedure for forming octadecylated surfaces was designed for hot-embossed poly(methyl methacrylate) (PMMA) devices [14]. First, the surface methyl ester groups of the polymer were converted into amines by reaction with *N*-lithioethylenediamine. Then, the channels were filled with octadecylisocyanate, which reacted with pendant amine functionalities to afford a C_{18}-modified surface. It is worth noting that this procedure resulted in a positively ionized surface as a result of residual, unreacted surface amine groups. This charged surface caused electroosmotic flow to run from cathode to anode. Using surface-modified PMMA devices with 85 μm deep and 15 μm wide channels, the reversed-phase separation of a low mass sizing ladder of double-stranded DNA fragments was achieved in the presence of triethylammonium acetate (TEAA), which acted as an ion-pairing agent [14,15].

The same type of device was later used to carry out the separation of two DNA fragments produced via the polymerase chain reaction (PCR) of λ-DNA [16]. A comparison of the retention times of the two PCR products with those from a similar separation of a DNA sizing ladder afforded qualitative agreement with the expected size of the PCR products (Fig. 5). The DNA sizing ladder, which contained six DNA fragments ranging in size from 100 to 2000 base pairs, was nearly baseline-resolved with an efficiency on the order of 10^4 plates for a 3 cm long column. Although the positively charged PMMA surface and the resulting "reversed" EOF helped to elute the negatively charged DNA fragments quickly, separation efficiency might have been even higher were it not for the undesirable electrostatic interactions between the DNA and the surface. It should be noted that, rather than using laser induced fluorescence detection, DNA peaks were monitored using bipolar pulse contact conductivity detection, which does not require fluorescently labeled analytes [15]. The basic requirement for conductivity detection is a sufficient difference in conductivity between migrating analyte zones and the mobile phase buffer.

Open channel chips have also been prepared from unsaturated alcohol-modified polyester resins. Rather than

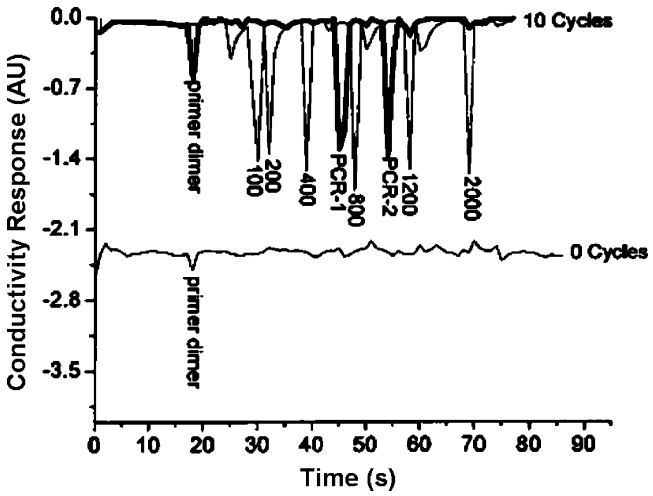

Fig. 5. Reversed-phase ion-pair OChEC separation of a DNA low mass sizing ladder (100 ng/mL) and PCR product profiles at 0 PCR cycles and 10 PCR cycles using a C_{18}-modified PMMA microdevice. The sizing ladder consisted of 100, 200, 400, 800, 1200 and 2000 base pair (bp) fragments. The primer dimer peak along with the 500-bp (PCR-1) and 1000-bp (PCR-2) product peaks are shown as the thick dark line. The separation was accomplished using 25 mM TEAA (ion-paring agent, pH 7.4) with a mobile phase composition comprised of acetonitrile–water (15:85, v/v) at a field strength of 67 V/cm. Detection was carried out using contact conductivity detection. The conductivity cell was operated at 5.0 kHz and a pulse amplitude of −0.5 V. From Ref. [16] with permission.

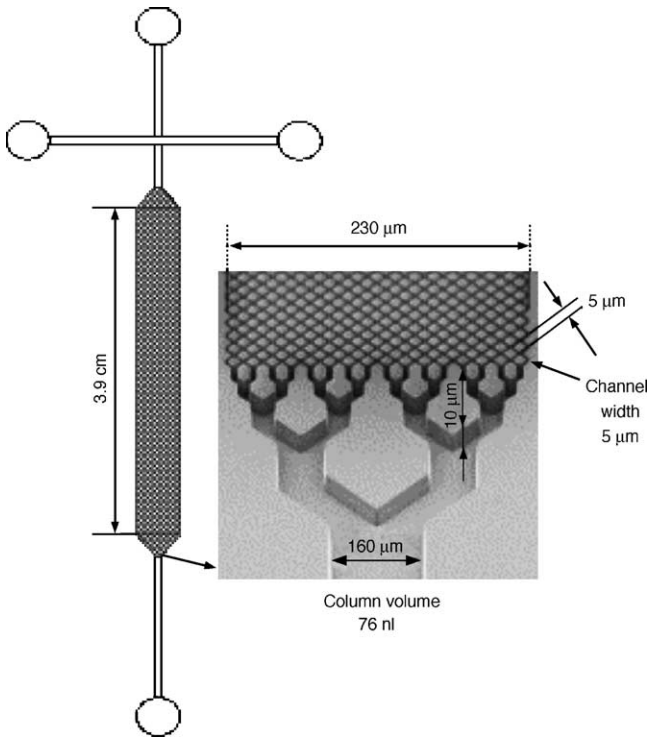

Fig. 6. Layout of a typical COMOSS separation column and an SEM image showing the microfabricated inlet splitter. From Ref. [23] with permission.

performing a surface modification of the final chip, straight-chain unsaturated alcohols, such as 10-undecene-1-ol, were included in the polyester mixture prior to its curing, so that the alcohol was incorporated in the crosslinked polymer structure. The alcohol chains were therefore located not only on the surface of the channels, but also within the bulk of the device. The initial demonstration of a reversed-phase separation of two sulforhodamine dyes in an undecenol-modified channel afforded significantly improved resolution compared to a purely electrophoretic separation in a fused silica capillary [17]. A detailed study on the effect of alkyl chain lengths of the incorporated alcohols (C_5, C_8, and C_{11}) and the effect of varying the undecene-1-ol concentration revealed a decrease in separation performance with increasing alkyl chain length. In fact, the best resolution was obtained with the native polyester, thus rendering all modification efforts questionable [18]. Although still unoptimized in this study, the concept of bulk, rather than surface modification, might prove useful with other functional moieties and polymers.

3. Microfabricated support structures

Taking advantage of the ability to fabricate small, highly regular structures using micromachining techniques, Regnier and coworkers have developed a new type of chromatographic column that does not fit the traditional definitions of either open channel or packed bed columns [19–25]. The microfabricated channels he used contained so-called collocated monolith support structures (COMOSS), which are essentially a tightly packed array of posts (Fig. 6). The size and shape of the posts, as well as the dimensions of the channels between them, can be varied as desired. Although the support structures are called directly fabricated “particles,” the resulting column is referred to as “a bundle of interconnecting capillaries with frequent mixing nodes” [24]. COMOSS have numerous advantages, including the uniformity and regularity of the support particles, the high level of control over the channel dimensions and geometry, and the ability to control the extent of mixing in the column. Compared to open channel columns, COMOSS columns posses surface areas larger by a factor of two to three, and hence higher loading capacities. The open channel devices discussed above require the use of very shallow channels to counteract the slow mass transfer in liquids and achieve high efficiencies. However, such shallow channels can be plugged easily with sample impurities, and they exhibit an extensive resistance to flow, which results in high pressure drops during pumping. Finally, unless special means are applied, the very short optical detection path makes on-chip detection difficult. In contrast, channels in COMOSS devices can be larger since the spacing of support structures, not the total channel height, controls the separation performance. Further, microfabricated support structures do not require retaining frits or complicated packing procedures, which are required in order to pack channels with beads.

The initial reports on COMOSS columns primarily investigated the design and fabrication of the devices [19,20]. Anisotropic deep reactive ion etching was utilized in order to create small, high aspect ratio support structures in quartz devices. The 150 μm wide and 4.5 cm long separation channel contained 5 μm × 5 μm diamond-shaped posts that were 10 μm high and separated by 1.5 μm wide rectangular channels. The channels were designed to have a constant cross-sectional area, even through the separation section, so that a constant linear velocity would be maintained and the possibility of bubble formation minimized.

The stationary phase was created on the internal surfaces of the device using a two-step procedure. First, the channel walls were silanized with (3-aminopropyl)triethoxysilane. Then, poly(styrene sulfonate) was electrostatically attached to the amine-modified surface to create a hydrophobic coating suitable for the reversed-phase separation mode. An efficiency of 35 000 plates per chip (777 000 plates/m) was determined with rhodamine 123 [19,20]. In a related study, quartz chips of the same design were used for reversed-phase ChEC of the FITC-labeled tryptic digest of ovalbumin [21]. Instead of electrostatically coated polystyrene sulfonate, the stationary phase in this chip consisted of a C_{18}-modified surface. The performance of this COMOSS device was compared to both an electrophoretic separation of the same digest on a COMOSS chip without stationary phase and to a gradient separation of unlabeled ovalbumin digest performed on a conventional 4.6 mm HPLC column confirming the separation advantage of COMOSS desigin.

A drawback of these devices is their high cost as the cost of each quartz COMOSS device has been estimated to be as high as US$ 2000 [26]. Further implementation of the design was therefore carried out using poly(dimethylsiloxane) (PDMS) microchips, which can be rapidly and inexpensively fabricated using replica molding [22–25]. However, due to the mechanical properties of PDMS and the fabrication technique used, these collocated monolith support structures typically have larger dimensions and spacing, as well as a lower aspect ratio, than those microfabricated in quartz. The first PDMS chips had a 3.9 cm long compartment containing 10 μm × 10 μm diamond-shaped posts with 5 μm spacing [22,23]. The post structures had slightly sloped walls and their dimensions ranged from 9.8 μm wide at the top of each post to 12.3 μm wide at the base, with channel widths impacted accordingly. These posts were coated with two different chemistries. First, a covalently bound coating of either C_8 or C_{18} alkyl chains was created by silanization of oxygen plasma-treated PDMS with the appropriate alkyl silane. Although separations featuring high efficiencies were achieved, alkyl silane coatings significantly reduced electroosmotic flow because the surface modification decreased the number of silanol groups driving EOF. It is worth noting that the decrease in EOF after coating the PDMS surface with octadecylsilane was much larger than the 10–25% decrease reported for similar treatment of glass microchannels [10]. To alleviate this problem, 0.2% sodium dodecylsulfate (SDS) was added to the mobile phase [22]. Alternatively, an electrostatically-attached layer of polystyrene sulfate was applied using the procedure described above.

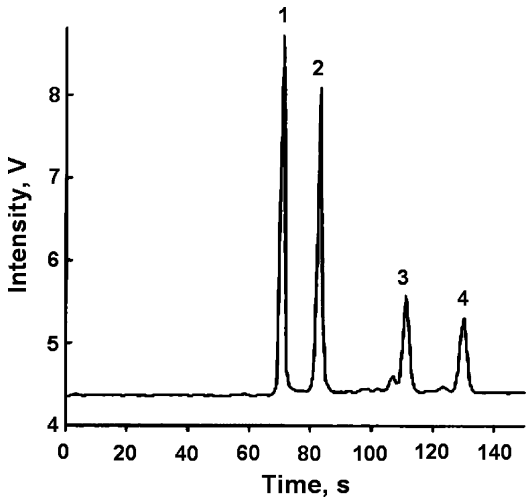

Fig. 7. Reversed-phase separation of FITC-labeled peptides on a C_{18}-AMPS modified PDMS COMOSS microchip. Electrokinetic injection, 1000 V for 0.25 s; mobile phase, 1 mM carbonate buffer (pH 9.0); applied voltage, 3000 V; fluorescence detection; analytes, (1) FITC–Gly–Phe–Glu–Lys(FITC)–OH; (2) FITC–Gly–Phe–Glu–Lys–OH; (3) FITC; (4) FITC–Gly–Tyr–OH. From Ref. [23] with permission.

In another study, ionizable polymeric stationary phases were grafted onto the walls of the oxidized COMOSS surfaces via free radical polymerization, using cerium(IV) as a catalyst. The charged polymer coatings were capable of supporting EOF while simultaneously providing a hydrophobic surface suitable for chromatography. Although the polymer coatings were initially thought to attach to the PDMS walls through siloxane bonds, the authors suggested that they were quickly hydrolyzed in the basic buffer that was used as the mobile phase. The authors hypothesized that the coatings became physically adsorbed onto the PDMS surface, and thus remained in place. A variety of monomers were investigated for creating the coated polymer stationary phase, including vinylsulfonic acid, acrylic acid, 4-styrenesulfonic acid, and 2-acrylamido-2-methyl-1-propanesulfonic acid (AMPS). Coatings made from AMPS afforded the best results with a test mixture comprising fluorescein isothiocyanate (FITC)-labeled peptides, achieving both high efficiency and reproducibility. In order to further increase hydrophobicity of the stationary phase, devices already coated with AMPS were additionally silanized with methoxydimethyloctadecylsilane. Fig. 7 illustrates the performance of a C_{18}-AMPS modified device; efficiencies were as high as 24 180 plates/chip (620 000 plates/m). A copolymer of AMPS and stearyl methacrylate was also investigated as an alternative way to achieve increased hydrophobicity via a single step procedure; however, these coatings were difficult to prepare and efficiencies were low.

Taking further advantage of the ability to control the size, shape, and dimensions of the microfabricated columns,

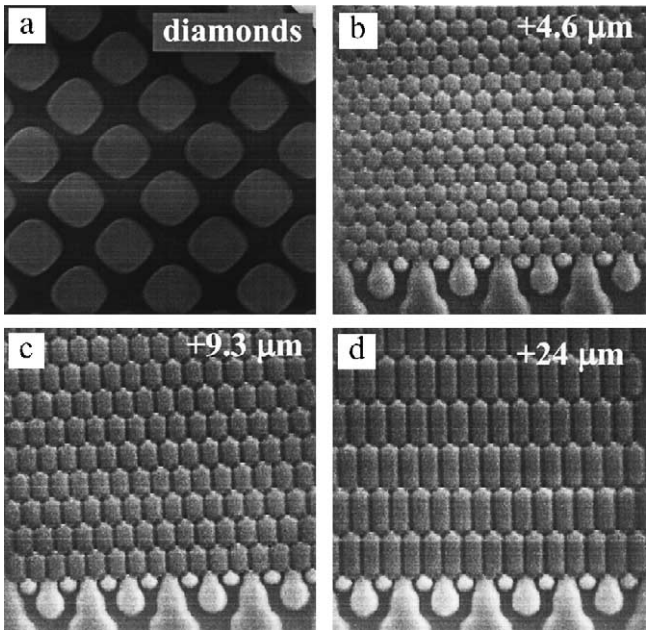

Fig. 8. SEM images of PDMS COMOSS columns with typical diamond-shaped posts (a) and extended hexagonal modifications with extension lengths of 4.6 μm (b), 9.3 μm (c), and 24 μm (d). From Ref. [24] with permission.

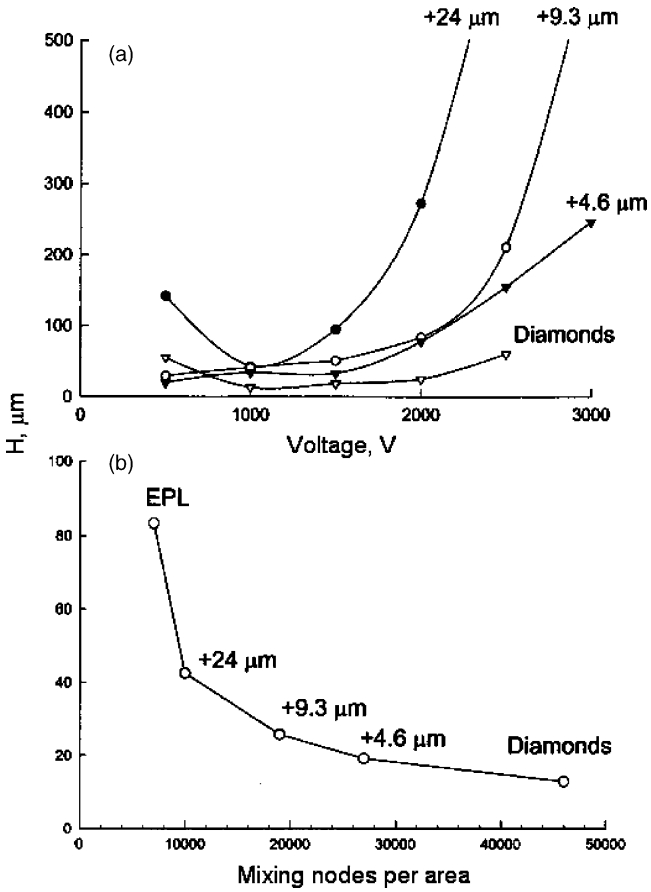

Fig. 9. Plots of (a) plate height (H) vs. voltage and (b) minimum plate height (H) vs. mixing nodes per area for the COMOSS columns shown in Fig. 8. Channel surfaces were modified with poly(4-styrenesulfonic acid). Mobile phase consisted of 1 mM sodium hydrogencarbonate–potassium carbonate buffer (pH 9.0). Model compound was rhodamine 110. From Ref. [24] with permission.

the effects of geometry on the performance of COMOSS columns made from PDMS were also investigated [24]. First, the size and spacing of the posts were varied: support structures of 11.1 μm × 11.1 μm diamond shapes with 3.9 μm spacing were compared to 5.5 μm × 5.5 μm diamond structures with either 2.5 or 4 μm spacing. Devices with these three different COMOSS designs were fabricated with channel depths of 1.6, 2.6, 5.6, and 10 μm. The 1.6 and 2.6 μm deep devices were not functional because the flexibility of the PDMS allowed the cover slab to effectively form a seal to the bottom of the channels, thus blocking fluid flow through the column. The electrochromatographic studies with the remaining devices were carried out using C_{18}-AMPS coatings as the stationary phase. As expected, the performance of the devices improved as the size and spacing of the support structures decreased. However, the smallest and most closely spaced structures (10 μm tall, 2.5 μm spaced 5.5 μm × 5.5 μm diamonds) were flexible enough to allow the posts to bend and touch their neighbors. This increased the heterogeneity of the structure and led to poorer performance.

This study also explored the importance of interchannel mixing by varying the number of intersections of streams in the COMOSS column. Thus, the standard diamond shape of the support structures was extended by 4.6, 9.3, and 24 μm to form hexagonal structures (Fig. 8). Clearly, the longer the hexagonal support structures, the fewer mixing points per unit area. As Fig. 9 shows, the efficiency of these devices decreased exponentially with decreasing interchannel mixing. The authors state: "... these results suggest that even though the COMOSS system seems to be very homogeneous there is substantial heterogeneity in the system" [24]. They also suggest that the surface roughness of the channel walls may force fluid to pass through the channels between support structures at different velocities. Fluid in the diamond-shaped COMOSS is mixed frequently and small differences in channel velocity are unimportant. However, mixing in devices with long hexagonal posts is less frequent and band broadening is significant. Another surprising discovery was made by comparing COMOSS fabricated from different types of molds. Positive photoresist molds afforded structures with a much lower aspect ratio than those made using plasma-etched silicon masters. However, the lower aspect ratio structures had a much better efficiency than their high-aspect ratio counterparts. The low-aspect ratio structures performed better probably due to both their smaller effective channel diameters, which improves mass transfer, and to the absence of sharp rectangular corners, where stagnant pools can develop.

The most recent ChEC device from the same group included not only a COMOSS separation column, but also packed beds for both enzymatic digestion and immobilized

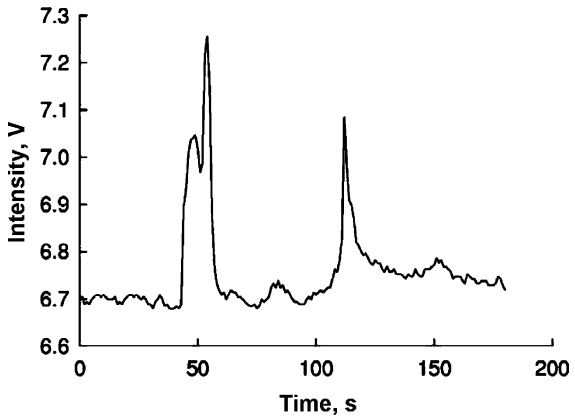

Fig. 10. A reversed-phase ChEC separation of FITC-BSA after on-chip trypsin digestion and Cu(II)-IMAC selection. Trypsin digestion was performed in continuous flow mode. Peptides were eluted from the Cu(II)-IMAC column with a plug of eluting buffer (20 mM phosphate with 0.5 M NaCl and 1 M EDTA, pH 9.0). Separation was performed on an AMPS-modified COMOSS column using 1 mM phosphate running buffer (pH 7.0) and a field strength of 500 V/cm. From Ref. [25] with permission.

metal affinity chromatography (IMAC) [25]. This device was designed to digest a protein, selectively capture the histidine-containing peptides from the digest mixture, and then separate the isolated peptides using reversed-phase electrochromatography. All operations were performed using electroosmotically-driven flow. Although the 4 cm separation channel contained collocated monolith support structures, the other two operations were performed on short packed beds of functionalized beads. Silica beads were used because they could be functionalized using standard procedures, as opposed to developing new techniques that would be required for surface modification of PDMS COMOSS structures. The 5 μm beads, containing either immobilized trypsin or iminodiacetic acid groups loaded with copper(II), were electrokinetically packed in the chip and retained there by microfabricated COMOSS-like frits. A reversed-phase polymer coating of AMPS on the COMOSS separation column was prepared using the procedure developed earlier. The 10 μm tall support structures of both the separation column and the frits were 5 μm × 5 μm diamonds with 3 μm spacing. The performance of the IMAC and enzymatic digestion units were first tested separately. Then, using reduced and alkylated FITC-labeled bovine serum albumin (FITC-BSA) as a substrate, all the steps of the integrated system were demonstrated together, including digestion, selection, and separation. The resulting chromatogram, shown in Fig. 10, contained three major peaks detected by laser induced fluorescence; however, trypsin digestion of BSA with no missed cleavages should produce 17 histidine-containing peptides. The small number of peaks was attributed to the use of FITC-labeled BSA rather than the native protein. The FITC-BSA contained, on average, 12 FITC labels attached randomly to lysine residues. Since trypsin cleaves proteins on the C-terminal side of lysine and arginine residues and does not cleave the labeled residues, trypsin digestion of FITC-labeled BSA would be expected to be incomplete. Digestion of unlabeled BSA followed by on-chip labeling or mass spectrometry (MS) detection may help to avoid incomplete digestion. However, the latter was not possible in this case due to severe “bleeding” of polymer from the PDMS device [27,28].

4. Channels packed with particles

While COMOSS microchips have a much larger surface area than similar, open channel devices, even higher phase ratios can be achieved in channels packed with beads [21]. In addition to their large surface area, conventional silica-based stationary phases are widely available, well characterized, and easily functionalized. However, packing them uniformly and reproducibly in the channels of a microchip represents a significant technical challenge [29]. Another key obstacle to the use of beads is the need to include frits or other retaining structures within the microchannels.

Oleschuk et al. [30] have developed a simple glass microfluidic chip for solid-phase extraction and electrochromatography in which beads were trapped between two microfabricated weirs. To pack the channel, a slurry of ∼1.5 μm octadecylsilica particles in acetonitrile was electroosmotically pumped through a narrow side channel into a 10 μm deep and 200 μm long chamber. Particles were retained between two 9 μm high weirs (Fig. 11). During solid-phase extraction experiments, concentration enhancement factors up to 500 were achieved; however, the separation performance of this very short bed for two fluorescent dyes was limited to an efficiency of 50 000–100 000 plates/m, or a plate height of 20–10 μm. The low efficiencies were due in part to the fact that the packed bed was locked in place only by hydrophobic interactions between the beads. Repeated runs caused particles to dislodge, creating voids in the bed. In addition, using mobile phases with high percentages of acetonitrile reduced the strength of the agglomeration, destabilizing the bed further [31].

The performance, stability, and lifetime of the microchip described above have been improved by physically entrapping the beads in the chamber with a thermally initiated monolithic poly(ethylene dimethacrylate) plug immediately after their packing [31]. The use of polymer plugs led to significantly improved separation performance. Efficiencies up to 84 plates/chip (420 000 plates/m) and 23 plates/chip (115 000 plates/m) were achieved for acridine orange and BODIPY, respectively. This device was also successfully used for the separation of alexafluor-labeled angiotensin II from excess of the dye.

Further improvements in chromatographic performance were demonstrated using quartz microchips with separation channel lengths of 1, 2, and 5 mm [32]. In order to achieve void-free packing in these longer columns, octadecylsilica

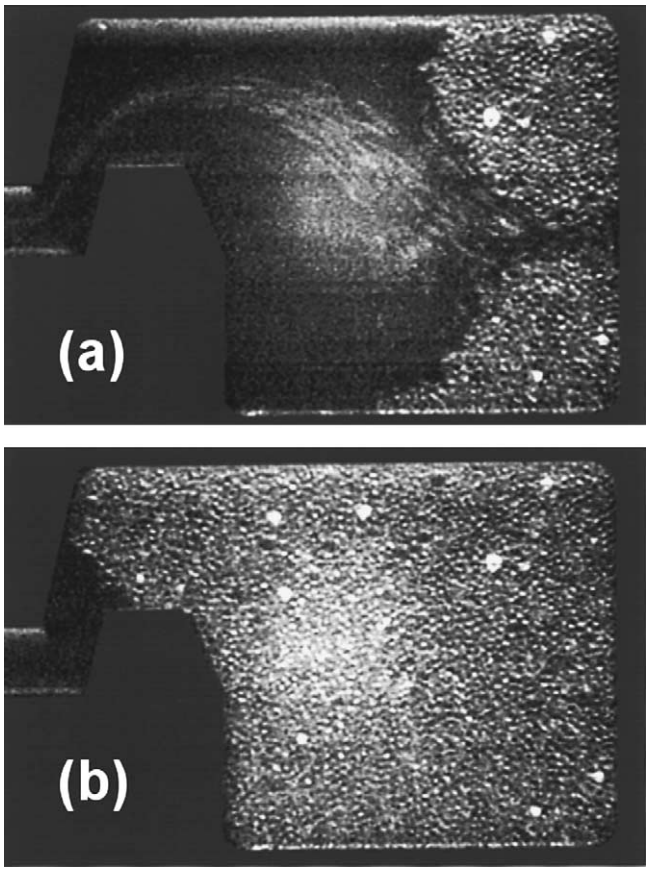

Fig. 11. Images of a 200 μm long microfabricated bead chamber (a) at an initial stage of electrokinetic packing and (b) after it was completely filled with beads. Image background was colored to enhance contrast. From Ref. [30] with permission.

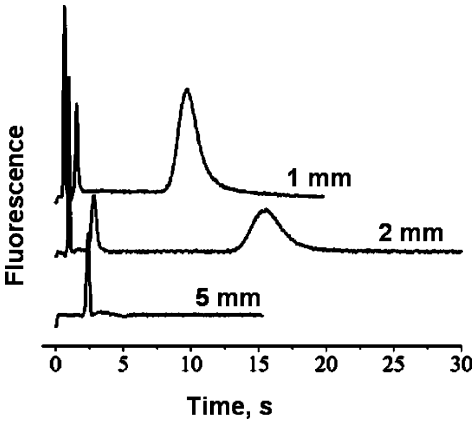

Fig. 12. Electrochromatograms showing separations at 2 kV on three column lengths of packed octadecylsilica beads. Injection was performed for 10 s, at −1 kV. The dyes eluted in the order BODIPY, rhodamine 123 and acridine orange (AO). Mobile phase was 80% ACN and 20% 25 mM Tris–HCl, pH 8.0. Column lengths are indicated. Traces are slightly offset, fluorescence intensity scales differ for each trace. *Conditions*: 1 mm column, 600 V photomultiplier tube (PMT) bias, 10 nM BODIPY, 12 nM rhodamine 123, 8 nM AO; 2 mm column, 550 V PMT bias, 6 nM in each dye; 5 mm column, 550 V PMT bias, 6 nM BODIPY with no other dyes. From Ref. [32] with permission.

beads were packed using mechanical pumping in addition to electroosmotic flow. As before, the packed beads were fixed in place with a polymer plug, though in this study polymerization was photoinitiated. Although stable 1 and 2 mm beds could be formed with this technique, only about one-third of the 5 mm beds performed reliably void formation. Not surprisingly, separations on these columns afforded much higher plate numbers than the 200 μm long column used in the previous study. The chromatograms in Fig. 12 compare the separations of fluorescent dyes on the chips with different column lengths. The 1 mm column produced up to 330 plates (330 000 plates/m), and the 2 mm long column yielded about 1.8 times more theoretical plates than the 1 mm column. However, the performance and reproducibility of the 5 mm column were poor. This emphasizes the fact that efficient packing of long beds in microfluidic channels is very difficult. This study also successfully demonstrated indirect detection for a mixture of two unlabeled amino acids using 8–10 nmol/L BODIPY in the running buffer.

Ceriotti et al. [33] fabricated a fritless packed column for reversed-phase ChEC in a PDMS device. Rather than use weirs or frits, the 70 μm wide and 30 or 50 μm deep separation channel was tapered to a width of 16 μm over a length of 0.5–1 mm. To pack the column, vacuum and pressure were applied to drive an acetone slurry of 3 μm octadecylsilica beads through the separation channel. At the taper, the density of particles increased and blocked the channel. This “keystone effect” supported and locked in place the rest of the particles. In order to stabilize the bed, the packed channel was annealed at 115 °C overnight. Without this thermal treatment, the bed was not stable and the formation of voids was observed during its use. It is likely that the thermal treatment fused the beads together and possibly also to the channel walls, forming a stable quasi-monolithic structure; similar treatments have been used in capillary electrochromatographic studies [34–36]. The ChEC capabilities of a 1.7 cm long packed column were demonstrated with a 15 s baseline separation of methanol and benzaldehyde. The mobile phase contained 1 mmol/L sodium fluorescein for indirect detection. The efficiency was 4930 plates (290 000 plates/m) and 2040 plates (120 000 plates/m) for methanol (unretained) and benzaldehyde, respectively. While these results appear promising, the usefulness of the device was significantly limited due to problems with the substrate material including absorption of some of the analytes by the PDMS. As a result, most chips could only be used for a single day. The column-to-column reproducibility was poor most likely due to differences in packing length and to the instability of the oxidized PDMS surfaces that were required to achieve enhanced wettability. The use of a different surface modification procedure and/or polymer substrate material might resolve some of these issues.

Polyelectrolyte multilayers have since been investigated in order to improve the performance of PDMS devices for packed bed ChEC [37]. Dynamic coatings of polyelectrolyte

multilayers were chosen in order to overcome some of the disadvantages of PDMS, such as the tendency of PDMS surfaces to absorb analytes and the instability of electroosmotic flow in oxidized PDMS channels. This approach was demonstrated with multilayers of cationic polybrene and anionic dextran sulfate in PDMS microchannels and led to stable EOF over a wide pH range [38]. In this study, a polyelectrolyte double layer was produced by simply filling the channel with an aqueous solution of polybrene followed by an aqueous solution of dextran sulfate. Using this approach, absorption of neutral analytes was significantly reduced [37]. However, the layers had limited stability, and the device could only be used for about 1 h. To perform reversed-phase electrochromatography, a 3 mm long separation column was hydrodynamically packed with 5 μm octadecylsilica particles that were retained within the column by microfabricated structures similar to those used in COMOSS devices [25] with a difference that microfabricated frits were created at both ends of the column. Another feature is that the cross-sectional area of the channel in the frit region was not kept constant. While the separation chamber was 150 μm wide, the inlet and outlet channels were only 50 μm wide. In addition, the microfabricated frits appear to be asymmetrical, which would likely result in poorly swept regions in-between the post rows and thus lead to band broadening. Preconcentration and electrochromatography of two coumarin dyes were performed on this device. Preconcentration of the dyes at the front end of the column during sample loading was followed by elution and separation. While no efficiency data was reported, the coumarin peaks were baseline resolved with moderate efficiencies.

Sol–gel immobilization of silica particles, described in detail elsewhere in this issue, has very recently been utilized as another technique for the fritless packing of microchannels [39]. A stationary phase was formed at defined locations in a quartz microchip prior to bonding the cover plate. The location of the stationary phase was controlled using a small, reversibly bonded PDMS slab. Only the sections of microchannel covered by this slab were filled with the sol–gel reaction mixture that contained 5 μm C_4 silica beads. After the bed was formed, the small slab was removed and a PDMS cover plate was irreversibly bonded to the quartz wafer. A reversed-phase electrochromatographic separation of three dipeptides was demonstrated using isocratic conditions and UV absorbance detection.

5. Porous polymer monoliths

Polymer monolithic stationary phases have many of the same benefits as packed chromatographic beds, including high surface area and easily controlled surface chemistry. However, a distinct advantage of monolithic stationary phases is the ability to prepare them easily and rapidly via free radical polymerization within the channels of the microdevice without need for frits or other retaining structures. The porosity, surface area, and pore size of the monolith are controlled by adjusting the composition of the initial monomer solution and the polymerization conditions. A wide variety of chemistries can be introduced into the microfluidic device through appropriate selection of monomers.

The first polymer-based monolithic stationary phases were prepared in quartz microchannels. The serpentine channels etched into quartz substrates and sealed with a 4 μm thick layer of silicon dioxide were 30.6 cm long and approximately 40 μm wide and 20 μm deep [40]. Before formation of the polymer monolith, the channels were treated with [3-(methacryloyloxy)propyl]trimethoxysilane. During polymerization, pendant methacryloyl groups of the pretreated surface were incorporated into the growing polymer monolith, covalently attaching it to the channel walls. Monolithic stationary phase for reversed-phase electrochromatography was created by polymerization of methacrylamide, isopropyl acrylamide, piperazine diacrylamide (crosslinker), and vinylsulfonic acid mixtures in an aqueous buffer solution using the redox initiating system ammonium peroxosulfate–tetramethylethylenediamine (TEMED). In addition, similar polymerization mixtures were used to create polymer monoliths for pressure-driven anion-exchange liquid chromatography with the exception that diallyl dimethylammonium chloride was substituted for isopropyl acrylamide and vinylsulfonic acid. Polymerization began once the initiator was added, therefore the channels had to be filled immediately after the mixture was prepared.

The location of the polymer bed could be controlled to a limited extent by using fluid plugs containing poly(ethylene glycol) (PEG), TEMED, and ammonium peroxodisulfate but no monomers. These fluid plugs displaced the polymerization mixture to keep certain sections of the microchannel clear of monolith. The plugs also helped to create sharp ends to the monolith. The completed chips were attached to a special clamp apparatus for fluid interfacing and operated using a highly modified CE instrument capable of UV detection. This implementation required a laborious procedure for changing the contents in the inlet reservoir to achieve sample injection.

The performance of the monolithic stationary phase in the microchip was compared to that in a fused silica capillary. Not surprisingly, Van Deemter plots were virtually identical for both devices since the channel, which did not have on-chip injection arms, closely resembled a capillary etched in quartz. Neutral alkyl phenones and positively charged antidepressants were separated in the serpentine channel in 18 and 9 min, respectively. To demonstrate a faster separation, a Y-shaped channel geometry with a 1.8 cm long polymer monolith was used for a rapid separation of uracil, phenol, and benzyl alcohol. As shown in Fig. 13, the separation was completed in less than 20 s, with all three peaks eluting within a 7 s window. A separation efficiency of 6300 plates (350 000 plates/m) was found for the unretained analyte uracil.

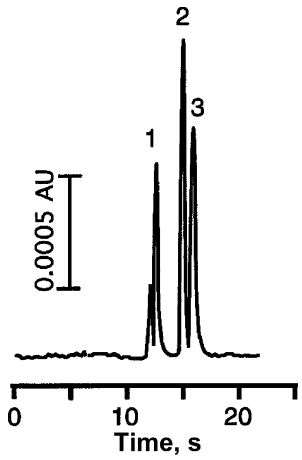

Fig. 13. Fast chip electrochromatography using a C_3^- porous polymer monolith with high EOF velocity. Straight column (18 mm effective length) × 40 μm width; mobile phase, 5 mM sodium phosphate, pH 7.4, containing 15% (v/v) acetonitrile; applied voltage, 2.4 kV (500 V/cm); EOF velocity, 2.1 mm/s. UV detection at 254 nm; electrokinetic injection, 100 V, 2 s. Sample: (1) uracil, (2) phenol, and (3) benzyl alcohol. From Ref. [40] with permission.

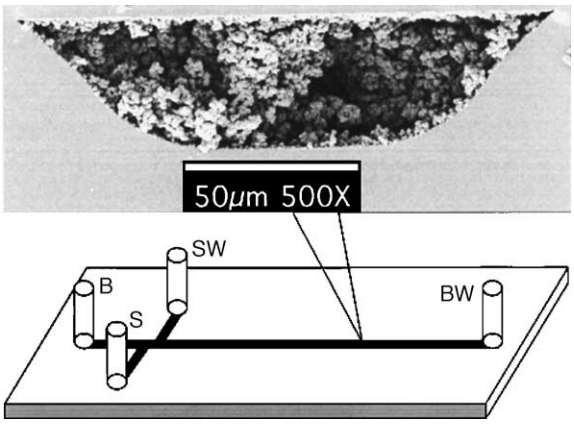

Fig. 14. Schematic of a typical microchip used for polymer monolith electrochromatography. B, S, BW, and SW denote reservoirs containing buffer, sample, buffer waste, and sample waste, respectively. The inset shows a scanning electron micrograph of a channel cross-section filled with photoinitiated acrylate polymer monolith. The mean pore diameter is 1 μm. From Ref. [54] with permission.

More recently, the same group developed a so-called hybrid microdevice as an alternative to the expensive and difficult to fabricate quartz microchips [41]. The hybrid device consisted of a short, fused silica capillary column set in a 0.4 mm groove on a poly(vinyl chloride) (PVC) substrate. The PVC support plate included sample reservoirs, electrodes, and a slit for "on-tube" UV-detection. In addition, a 2 mm diameter ball lens was mounted beneath the detection slit to focus the UV beam. The advantages claimed for this hybrid device in comparison to traditional microchips include lower cost in terms of materials and preparation, UV-detection with no need for fluorescent labels, the ability to change the separation column by simply switching the capillary, and the ability to directly utilize the existing body of experience available for capillary separations. However, the device is limited to very simple geometries and is less suitable for the more complex layouts typical of μ-TAS. Gel electrophoresis and electrochromatography were performed on 2.8 cm long polymer gels prepared from acrylamide and allyl-β-cyclodextrin crosslinker. AMPS (1%, w/v) was included in the polymerization mixtures of the polymer gels used for ChEC. Several alkyl phenones were separated in the electrochromatographic mode in less than 200 s. The suggested separation mechanism was related to interactions between the hydrophobic cavity of the β-cyclodextrin and the analytes. However, no direct evidence for this mechanism was presented.

In the late 1990s, we introduced UV initiated polymerization suitable for the preparation of monoliths within microfluidic devices such as capillaries and microchips [42,43]. Later we refined this approach to enable both the preparation of the monolith as well as its in situ surface functionalization [44–48]. The significant advantage of the photoinitiation approach is the ability to define photolithographically the size and position of the monolith using a mask through which the liquid polymerization mixture in the channel is irradiated. The process was demonstrated with the preparation of a variety of methacrylate-based monolithic porous polymer stationary phases. The typical polymerization mixtures contained monomers, initiator, and porogenic solvents. The monomer mixture contained crosslinkers such as ethylene dimethacrylate and trimethylolpropane trimethacrylate, and monovinyl monomers such as butyl methacrylate and AMPS. The initiator was originally 2,2′-azobisisobutyronitrile (AIBN). However, the use of aromatic phenone initiators enabled significant acceleration of the polymerization process such that it was completed in minutes as opposed to more than 12 h. A large number of various porogenic solvents were also tested [49].

A significant contribution to microfluidic ChEC with polymer based monolithic stationary phases originated from Sandia National Laboratories. Although their early studies primarily focused on the development of acrylate-based polymer monoliths in capillaries, initial test separations were also carried out on glass/fused silica microchips [50,51]. Fig. 14 shows a scanning electron microscopy (SEM) cross-section of a monolith-filled microchannel and a typical chip layout. Both positively charged and negatively charged monoliths were prepared using photoinitiated polymerization. Positively charged monoliths were found to be useful for separations at low pH since they enabled high EOF velocities and, at the same time, prevented unwanted electrostatic interactions with positively charged compounds, such as amine-containing compounds. A typical mixture comprised 1,3-butanediol diacrylate (crosslinker), butyl acrylate or combinations of butyl acrylate with lauryl acrylate, 0.5 wt.% ionizable monomer (AMPS for negatively charged monolith or [2-(acryloyloxy)ethyl]trimethylammonium methyl sulfate for positively charged monolith), 0.5%

(w/w) AIBN (photoinitiator), and 0.3% (w/w) adhesion promoter (z-6030, product of Dow Chemicals). The porogenic solvent contained ethanol, acetonitrile, and a phosphate buffer (pH 6.8). Capillaries and glass microchips were silanized using a surface pretreatment of [3-(methacryloyloxy)propyl]trimethoxysilane. Capillary action was used to fill the 50 μm wide and 25 μm deep microchannels with the liquid polymerization mixture and the monoliths were then prepared by exposure to UV light for 10–30 min. The ionized functionalities on the monolith enabled the use of electroosmotic flow, rather than pressure-driven flow, to purge the remaining reaction mixture from the porous material after polymerization. Three bioactive peptides fluorescently-labeled with naphthalene-2,3-dicarboxaldehyde (NDA) were separated using a 7 cm long monolithic stationary phase, affording efficiencies of 105–5800 plates (1500–83 000 plates/m). The performance was limited by undesirable electrostatic interactions of the peptides with the stationary phase [51].

The alkylacrylate-based monoliths were also used for the separation of polycyclic aromatic hydrocarbons. Good performance was demonstrated on the separation of three neutral PAHs with efficiencies of 8400–13 900 plates (140 000–231 000 plates/m) [50]. In a different study, the number of PAH analytes was increased to 13 [52]. In this study, the detection window was created by local degradation and removal of the monolith using the energy from a frequency-doubled argon ion laser, which was part of the laser-induced fluorescence detector. Depolymerization of the monolith in the desired window is simply effected by irradiating for 10–20 min while electroosmotically pumping fluid through the device.

Two different configurations of the polymer monolith were evaluated: (i) one in which all of the channels of the device were completely filled with porous polymer monolith and (ii) the other in which the monolith was polymerized only in a specific area of the chip as defined by a photolithographic mask. The photopatterned monolith in which all but the injection arms of the device were filled exhibited efficiencies of 100 000–150 000 plates/m as opposed to 180 000–200 000 plates/m for the chip completely filled with monolith. Heterogeneous regions in the patterned polymer, specifically at the ends of the monolith, and/or zeta potential mismatch were blamed for the poorer performance. Zeta potential mismatch between the sections of the chip with and without monolith might have introduced parabolic flow with concomitant band broadening and decreased efficiency. In addition to comparing their separation performance, the operational limitations and the reproducibility of the two types of monolithic devices were also investigated. For example, low resistance to flow in the device with open injection arms allowed running buffer to flow into the fluid reservoirs and dilute the sample during pinched separation runs [53]. On the other hand, injection times as long as 5 min or more were required to ensure uniform sample injections in the devices with monolith-filled

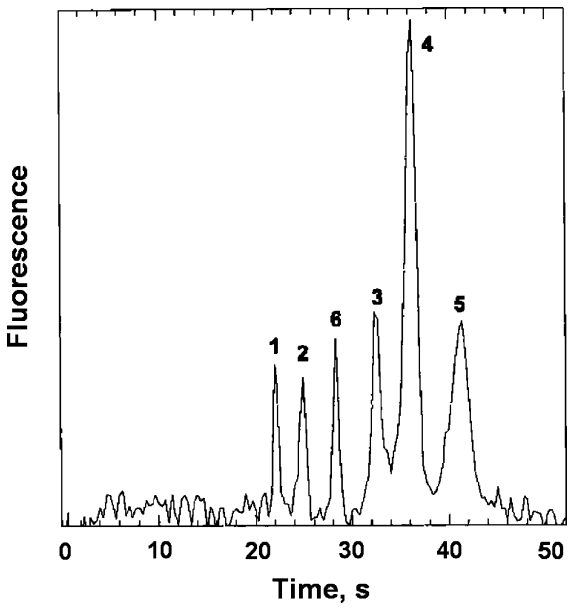

Fig. 15. Reversed-phase ChEC of peptides in a porous polymer monolith-filled microchip. The polymer was negatively charged lauryl acrylate monolith, peptides were labeled with NDA, and fluorescence detection was used. Field strength, 770 V/cm (5 kV); mobile phase, ACN–25 mM borate (pH 8.2) containing 10 mM octanesulfonate (30:70); analytes, (1) papain inhibitor, (2) proctolin, (3) opioid peptide (α-casein fragment 90-95), (4) Ile-angiotensin III, (5) angiotensin III, and (6) GGG. From Ref. [54] with permission.

sample arms. This study also highlighted the importance of carefully sealing the fluid reservoirs during chip operation. Using unsealed reservoirs, 95% reductions in signal peak heights were observed over the course of just five separations due to dissolved oxygen quenching the fluorescence of the PAHs. In addition, variations in retention times were rather high, with deviations up to 20%. Thus, further work was needed to improve the overall performance of these chips.

Microchips filled with acrylate-based polymer monolith were later used to separate bioactive peptides and amino acids [54]. Citing decreased performance due to zeta potential mismatch between open and monolith-filled channels, all the channels of the microchip were filled with monolith except for a small detection window. NDA-labeled peptides were separated with excellent efficiencies in fused silica chips with channels either 25 or 40 μm deep and 90–130 μm wide. The mobile phase contained 10 mmol/L octane sulfonate, apparently acting as an ion-pairing agent for the charged peptides [55]. The effect of voltage on the peptide separation was evaluated over the range from 1 to 5 kV. The best performance was obtained at 2 kV (∼300 V/cm), affording efficiencies of 127 000–600 000 plates/m (∼6350–30 000 plates/chip). However, even at the highest field strengths (770 V/cm), near baseline resolution was achieved and the separation was completed in 45 s (Fig. 15). A similar separation using the same acrylate monolith in a 100 μm i.d. fused-silica

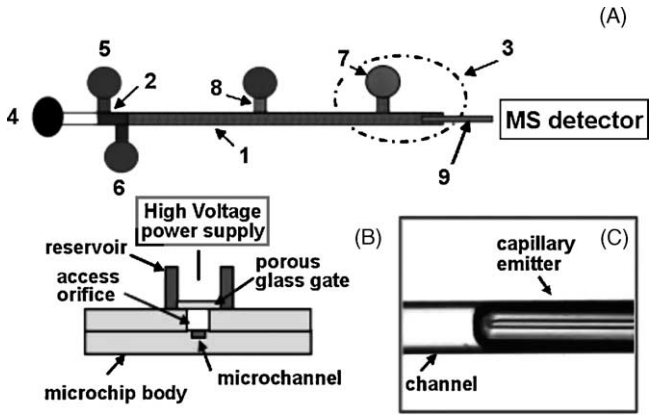

Fig. 16. (A) Schematic diagram of integrated polymer monolith ChEC microchip system with ESI-MS detection: (1) separation channel; (2) double-T injector; (3) ESI source; (4) eluent reservoir; (5) sample inlet reservoir; (6) sample waste reservoir; (7) eluent waste reservoir that houses a porous glass gate; (8) side channel for flushing the monolithic channel; (9) ESI emitter. (B) Cross-sectional view of reservoir 7, showing the position of the semipermeable glass gate. (C) Image of the on-chip junction between the separation channel and the ESI emitter. From Ref. [55] with permission.

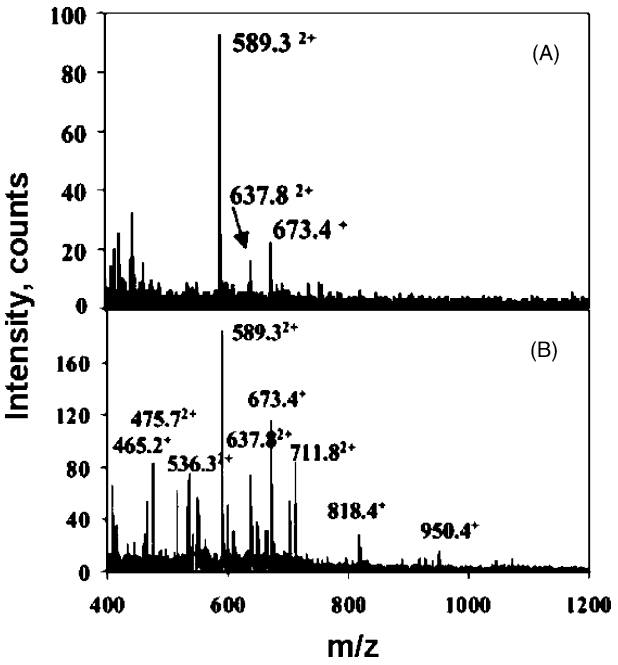

Fig. 17. Time-of-flight mass spectra of bovine hemoglobin tryptic digest: (A) separated peptides, eluted from the ChEC system; (B) unseparated peptides from an infusion experiment. *Separation conditions*: field strength, 350 V/cm; mobile phase, methanol–15 mM ammonium acetate (pH 4.6) (30:70); stationary phase, positively charged methacrylate-based polymer monolith. From Ref. [55] with permission.

capillary (23.5 cm to detection window, 303 V/cm) required more than 9 min to complete and produced only half as many plates. In contrast to the previous report [52], these new devices exhibited an improved reproducibility. RSD values for the retention times were approximately 2%. Since glass-based microchips are costly, this report also described a procedure for their recycling via thermal incineration of the monolith.

Lazar et al. [55] have recently demonstrated the first example of interfacing ChEC with mass spectrometric detection. The glass microchip contained a methacrylate-based monolith as well as an integrated capillary tip for electrospray ionization (ESI). The straight 130 μm wide and 50 μm deep main channel of the chip contained a 5–6 cm separation section that led directly to an ESI emitter (Fig. 16). A 5 mm long trench was etched into the cover plate before the chip was bonded to allow insertion of the emitter tip into the end of the separation channel. Further, the chip design included an additional fluid reservoir near the end of the separation channel. This reservoir contained a conductive, semipermeable glass disc, which allowed voltage to be applied to the fluid in the channel but prevented bulk fluid movement. With this design, electroosmotically driven fluid in the main channel was forced out through the ESI capillary tip. Similar to the Sandia approach [52,54], all of the microchannels were completely filled with monolith to ensure uniform EOF throughout the chip. The monolithic stationary phase was prepared by photoinitiated polymerization of mixtures consisting of glycidyl methacrylate, methyl methacrylate, and ethylene dimethacrylate in the presence of formamide and 1-propanol as a porogenic solvent and 2,2-dimethoxy-2-phenylacetophenone (DMPAP) as the initiator. Subsequently, the monolith was incubated with *N*-ethylbutylamine overnight at 70 °C. The amine reacted with the epoxy groups of glycidyl methacrylate on the monolith, forming tertiary amine functionalities and rendering the surface positively charged. This chemistry was chosen in order to minimize electrostatic interactions between the monolith and the positively charged peptides of bovine hemoglobin tryptic digest. Although it would also be possible to separate mixtures of peptides on negatively charged monoliths such as those prepared by copolymerization of AMPS, this approach would require the addition of an ion-pairing agent in the mobile phase. However, this approach is less useful since most ion-pairing agents are incompatible with ESI mass spectrometry.

The positively charged surface of the monolith caused the electroosmotic flow to run from cathode to anode. This EOF was opposite to the direction of electrophoretic migration of the analyzed peptides and increased the time required to travel through the relatively short column. Separations of the peptide mixture using mass spectrometric detection afforded a sequence coverage of 70–80% and efficiencies of 3000–4000 plates. While the tryptic digest was not completely separated on the monolithic stationary phase, the mass spectra were greatly simplified compared to a spectrum of the original peptide mixture (Fig. 17). In addition, multiplexed devices with three to four operating lines were also constructed.

However, a significant problem with this system involves sample injection. While the positively charged monolith and “reversed” EOF improved separation performance, they also

significantly enhanced electrophoretic discrimination during injection. In addition, despite the tuned chemistry, the analytes interacted with the amine functionalities and neutralized them, completely suppressing the EOF in the injection arms after multiple injections. This prevented long-term use of the device. Use of disposable, perhaps plastic, chips appears to be a simple solution to this problem.

6. Silica-based monoliths

Monolithic silica is the most recently introduced type of stationary phase for electrochromatography on microchips. Devices based on monolithic silica benefit from their very high surface area, adjustable pore size, and controllable surface chemistry. Functional moieties are typically incorporated onto the silica monolith by including an appropriate silicon alkoxide in the precursor mixture or by silanization of the surface after the monolith is formed. Monolithic silica-based columns are generally known to exhibit superior performance in the HPLC separation of small molecules, which is attributed to their large surface areas resulting from the presence of mesopores [56].

Silica monoliths in capillaries are usually prepared via acid catalyzed condensation of alkoxysilanes followed by heat treatment [57,58]. Thus, the spatial definition of such a monolith is difficult [12,40,59]. Zare and coworkers have developed a new method for the preparation of photopatternable sol–gel monoliths [60,61]. To create the monolith, they added a partially gelled solution of 3-methacryloxypropyltrimethoxysilane (MPTMS) to a mixture of photoinitiator in toluene shortly before filling the channels with this mixture via capillary action. Exposure to UV-light through a photomask initiated a free radical polymerization of the MPTMS. The resulting monolith was thus a hybrid between silica and polymer monoliths. The electrochromatographic performance of a 4.7 cm long monolith in a glass chip with 35 μm deep and 90 μm wide channels was demonstrated on the separation of two neutral coumarin dyes. Baseline resolution was achieved and efficiencies for the two peaks were 280 and 940 plates (6000–20 000 plates/m).

The Landers group also developed silica-based monolithic stationary phases suitable for microchip electrochromatography [26,62]. They modified a procedure originally developed by Ishizuka et al. [63]. First, an unmodified silica monolith was formed by hydrolytic condensation of tetramethyl orthosilicate in the presence of poly(ethylene oxide) (PEO). This water-soluble polymer induced a phase separation during gelation, resulting in a monolith with well-controlled porous properties. Varying its molecular weight significantly changed the resulting structure of the monolith and its chromatographic performance. The resulting monoliths were functionalized using two different procedures. First, a dynamically adsorbed cationic polymer poly(diallyldimethylammonium chloride) (PDDAC) was used to modify the monolith and make it suitable for anion-exchange electrochromatography [26]. To maintain the coating during separations, PDDAC was also included in the mobile phase. In the second approach, the silica monolith was coated with multiple, alternating layers of polymer electrolytes of opposite charges, which are referred to as polyelectrolyte multilayers (PEMs) [62]. The cationic layers in the PEM coating were made from PDDAC, while anionic layers consisted of either dextran sulfate or poly(styrene sulfate). This system afforded very stable and reproducible EOF. In addition, the multilayers could be used for multiple runs in ion-exchange and reversed-phase modes without the need for recoating. The use of dynamic or PEM coatings has several advantages over both modification with functional silanes and the use of silica precursors. For example, prior to modification by silanization the silica monolith must be completely dried. This drying process can lead to shrinkage or even cracking of the monolith. Next, although addition of functional alkoxysilanes to the monolith reaction mixture creates a functional monolith in a single step, the sol–gel process is more complex, and any attempt to adjust the composition of the monolith mixture may require redevelopment of the sol–gel process. With dynamic and PEM coatings, the monolith can be functionalized without prior drying and, further, the monolith formulation is decoupled from the coating formulation. However, application of this approach has yet to be demonstrated in microchips.

7. Conclusions

Chip electrochromatography is an attractive option for “lab-on-a-chip” separations due to its excellent separation performance and relative ease of implementation. Chip electrochromatography is readily adopted to a wide variety of substrate materials and types of stationary phases. Indeed, many types of stationary phases have already been developed in the 10 years since chip electrochromatography was first introduced. However, the most suitable stationary phase has not yet been determined. The choice of stationary phase will likely be application dependent, since each type of phase has its specific advantages and weaknesses. For example, although open channel phases suffer from low capacity, the ease of producing open channel coatings may make them attractive for some separations. Nonetheless, monolithic stationary phases appear to be the most versatile and robust type of stationary phase developed so far. Monoliths stand out because of their large surface areas, simple preparation, and wide choice of surface chemistries.

The field of chip electrochromatography is likely to continue to grow. Significant efforts have already been dedicated to creating and developing numerous viable options for the stationary phase. Now, the focus has shifted towards further improving separation performance. However, the development of new stationary phases is far from complete. In particular, silica-based monoliths are still in the early stages

of development. In addition, imprinted monolithic columns for chiral separations, which have been developed for capillary electrochromatography, may soon be transferred into the microchip format as well. Finally, another major area of development that is required to make ChEC affordable is related to the transition from expensive chips made from glass or quartz to inexpensive, mass-produced plastic devices while ChEC has been successfully demonstrated in plastic devices, it is clear that further development work is needed. Although much remains to be done, chip electrochromatography has a promising future in the development of μ-TAS.

References

[1] K. Seiler, Z.H.H. Fan, K. Fluri, D.J. Harrison, Anal. Chem. 66 (1994) 3485.
[2] G.J.M. Bruin, Electrophoresis 21 (2000) 3931.
[3] A. de Mello, Lab. Chip. 2 (2002) 48N.
[4] N. Lion, T.C. Rohner, L. Dayon, I.L. Arnaud, E. Damoc, N. Youhnovski, Z.Y. Wu, C. Roussel, J. Josserand, H. Jensen, J.S. Rossier, M. Przybylski, H.H. Girault, Electrophoresis 24 (2003) 3533.
[5] J.P. Kutter, Trends Anal. Chem. 19 (2000) 352.
[6] V. Kašička, Electrophoresis 24 (2003) 4013.
[7] F.E. Regnier, B. He, S. Lin, J. Busse, Trends Biotechnol. 17 (1999) 101.
[8] K. Mistry, I. Krull, N. Grinberg, J. Sep. Sci. 25 (2002) 935.
[9] S.C. Jacobson, R. Hergenröder, L.B. Koutny, J.M. Ramsey, Anal. Chem. 66 (1994) 2369.
[10] J.P. Kutter, S.C. Jacobson, N. Matsubara, J.M. Ramsey, Anal. Chem. 70 (1998) 3291.
[11] B.S. Broyles, S.C. Jacobson, J.M. Ramsey, Anal. Chem. 75 (2003) 2761.
[12] N. Gottschlich, S.C. Jacobson, C.T. Culbertson, J.M. Ramsey, Anal. Chem. 73 (2001) 2669.
[13] S. Constantin, R. Freitag, D. Solignac, A. Sayah, M.A.M. Gijs, Sens. Actuators B Chem. 78 (2001) 267.
[14] S.A. Soper, A.C. Henry, B. Vaidya, M. Galloway, M. Wabuyele, R.L. McCarley, Anal. Chim. Acta 470 (2002) 87.
[15] M. Galloway, W. Stryjewski, A. Henry, S.M. Ford, S. Llopis, R.L. McCarley, S.A. Soper, Anal. Chem. 74 (2002) 2407.
[16] M. Galloway, S.A. Soper, Electrophoresis 23 (2002) 3760.
[17] W. Xu, K. Uchiyama, T. Shimosaka, T. Hobo, J. Chromatogr. A 907 (2001) 279.
[18] W. Xu, K. Uchiyama, T. Hobo, Chromatography 23 (2002) 131.
[19] B. He, N. Tait, F. Regnier, Anal. Chem. 70 (1998) 3790.
[20] B. He, F. Regnier, J. Pharm. Biomed. Anal. 17 (1998) 925.
[21] B. He, J.Y. Ji, F.E. Regnier, J. Chromatogr. A 853 (1999) 257.
[22] B.E. Slentz, N.A. Penner, E. Lugowska, F. Regnier, Electrophoresis 22 (2001) 3736.
[23] B.E. Slentz, N.A. Penner, F.E. Regnier, J. Chromatogr. A 948 (2002) 225.
[24] B.E. Slentz, N.A. Penner, F. Regnier, J. Sep. Sci. 25 (2002) 1011.
[25] B.E. Slentz, N.A. Penner, F.E. Regnier, J. Chromatogr. A 984 (2003) 97.
[26] M.C. Breadmore, S. Shrinivasan, K.A. Wolfe, M.E. Power, J.P. Ferrance, B. Hosticka, P.M. Norris, J.P. Landers, Electrophoresis 23 (2002) 3487.
[27] N. Gottschlich, C.T. Culbertson, T.E. McKnight, S.C. Jacobson, J.M. Ramsey, J. Chromatogr. B 745 (2000) 243.
[28] Y.J. Liu, R.S. Foote, S.C. Jacobson, R.S. Ramsey, J.M. Ramsey, Anal. Chem. 72 (2000) 4608.
[29] G. Ocvirk, E. Verpoorte, A. Manz, M. Grasserbauer, H.M. Widmer, Anal. Meth. Instrument. 2 (1995) 74.
[30] R.D. Oleschuk, L.L. Shultz-Lockyear, Y.B. Ning, D.J. Harrison, Anal. Chem. 72 (2000) 585.
[31] A.B. Jemere, R.D. Oleschuk, F. Ouchen, F. Fajuyigbe, D.J. Harrison, Electrophoresis 23 (2002) 3537.
[32] A.B. Jemere, R.D. Oleschuk, D.J. Harrison, Electrophoresis 24 (2003) 3018.
[33] L. Ceriotti, N.F. de Rooij, E. Verpoorte, Anal. Chem. 74 (2002) 639.
[34] T. Adam, K.K. Unger, M.M. Dittmann, G.P. Rozing, J. Chromatogr. A 887 (2000) 327.
[35] R. Asiaie, X. Huang, D. Farnan, Cs. Horváth, J. Chromatogr. A 806 (1998) 251.
[36] M.M. Dittmann, G.P. Rozing, G. Ross, T. Adam, K.K. Unger, J. Cap. Electrophoresis 5 (1997) 201.
[37] K.W. Ro, W.J. Chang, H. Kim, Y.M. Koo, J.H. Hahn, Electrophoresis 24 (2003) 3253.
[38] Y. Liu, J.C. Fanguy, J.M. Bledsoe, C.S. Henry, Anal. Chem. 72 (2000) 5939.
[39] R. Jindal, S.M. Cramer, J. Chromatogr. A 1044 (2004) 277.
[40] C. Ericson, J. Holm, T. Ericson, S. Hjertén, Anal. Chem. 72 (2000) 81.
[41] Á. Végvári, S. Hjertén, Electrophoresis 23 (2002) 3479.
[42] C. Viklund, E. Ponten, B. Glad, K. Irgum, P. Horsted, F. Svec, Chem. Mater. 9 (1997) 463.
[43] C. Yu, F. Svec, J.M.J. Fréchet, Electrophoresis 21 (2000) 120.
[44] T. Rohr, E.F. Hilder, J.J. Donovan, F. Svec, J.M.J. Fréchet, Macromolecules 36 (2003) 1677.
[45] T. Rohr, D.F. Ogeltree, F. Svec, J.M.J. Fréchet, Adv. Funct. Mat. 13 (2003) 265.
[46] T.B. Stachowiak, T. Rohr, E.F. Hilder, D.S. Peterson, M. Yi, F. Svec, J.M.J. Fréchet, Electrophoresis 24 (2003) 3689.
[47] F. Svec, C. Yu, T. Rohr, J.M.J. Fréchet, in: J.M. Ramsey, A. van den Berg (Eds.), Micro Total Analysis Systems, Kluwer, Dordrecht, 2001, p. 643.
[48] F. Svec, J.M.J. Fréchet, E.F. Hilder, D.S. Peterson, T. Rohr, in: Y. Baba, A. van den Berg (Eds.), Micro Total Analysis Systems, Kluwer, Dordrecht, 2002, p. 332.
[49] C. Yu, M. Xu, F. Svec, J.M.J. Fréchet, J. Polym. Sci. Polym. Chem. 40 (2002) 755.
[50] S.M. Ngola, Y. Fintschenko, W.Y. Choi, T.J. Shepodd, Anal. Chem. 73 (2001) 849.
[51] R. Shediac, S.M. Ngola, D.J. Throckmorton, D.S. Anex, T.J. Shepodd, A.K. Singh, J. Chromatogr. A 925 (2001) 251.
[52] Y. Fintschenko, W.Y. Choi, S.M. Ngola, T.J. Shepodd, Fres. J. Anal. Chem. 371 (2001) 174.
[53] S.C. Jacobson, R. Hergenröder, L.B. Koutny, R.J. Warmack, J.M. Ramsey, Anal. Chem. 66 (1994) 1107.
[54] D.J. Throckmorton, T.J. Shepodd, A.K. Singh, Anal. Chem. 74 (2002) 784.
[55] I.M. Lazar, L.J. Li, Y. Yang, B.L. Karger, Electrophoresis 24 (2003) 3655.
[56] N. Tanaka, H. Kobayashi, N. Ishizuka, H. Minakuchi, K. Nakanishi, K. Hosoya, T. Ikegami, J. Chromatogr. A 965 (2002) 35.
[57] Z. Deyl, F. Svec (Eds.), Capillary Electrochromatography, Elsevier, Amsterdam, 2001.
[58] N. Tanaka, H. Kobayashi, in: Z. Deyl, F. Svec (Eds.), Capillary Electrochromatography, Elsevier, Amsterdam, 2001.
[59] L. Xiong, F.E. Regnier, J. Chromatogr. A 924 (2001) 165.
[60] M.T. Dulay, J.P. Quirino, B.D. Bennett, M. Kato, R.N. Zare, Anal. Chem. 73 (2001) 3921.
[61] K. Morishima, B.D. Bennett, M.T. Dulay, J.P. Quirino, R.N. Zare, J. Sep. Sci. 25 (2002) 1226.
[62] M.C. Breadmore, S. Shrinivasan, J. Karlinsey, J.P. Ferrance, P.M. Norris, J.P. Landers, Electrophoresis 24 (2003) 1261.
[63] N. Ishizuka, H. Minakuchi, K. Nakanishi, N. Soga, H. Nagayama, K. Hosoya, N. Tanaka, Anal. Chem. 72 (2000) 1275.